Eur. Phys. J. C 31, 187–196 (2003)
Digital Object Identifier (DOI) 10.1140/epjc/s2003-01319-9

THE EUROPEAN PHYSICAL JOURNAL C

Comparing the QCD potential in perturbative QCD and lattice QCD at large distances

S. Recksiegel[1], Y. Sumino[2]

[1] Theory Group, KEK, Tsukuba, Ibaraki, 305-0801 Japan*
[2] Department of Physics, Tohoku University, Sendai, 980-8578 Japan

Received: 15 April 2003 / Revised version: 15 July 2003 /
Published online: 2 October 2003 –

Abstract. We compare the perturbatively calculated QCD potential to that obtained from lattice calculations in the theory without light quark flavours. We examine $E_{\rm tot}(r) = 2m_{\rm pole} + V_{\rm QCD}(r)$ by re-expressing it in the $\overline{\rm MS}$ mass $\overline{m} \equiv m^{\overline{\rm MS}}(m^{\overline{\rm MS}})$ and by choosing specific prescriptions for fixing the scale μ (dependent on r and $\overline{m}$). By adjusting $\overline{m}$ so as to maximise the range of convergence, we show that perturbative and lattice calculations agree up to $3\,r_0 \simeq 7.5\,{\rm GeV}^{-1}$ (r_0 is the Sommer scale) within the uncertainty of order $\Lambda_{\rm QCD}^3\, r^2$.

1 Introduction

For decades, the static QCD potential $V_{\rm QCD}(r)$, formally defined from an expectation value of the Wilson loop, has been widely studied for the purpose of elucidating the nature of the interaction between heavy quark and antiquark. In modern language, a link to physical reality can be made naturally in the frame of potential–non-relativistic QCD (potential–NRQCD) formalism [1–3], in which $V_{\rm QCD}(r)$ is identified with the leading potential in an expansion in $1/m$ of the heavy quarkonium system. Therefore, $V_{\rm QCD}(r)$ dictates, for instance, the bulk of the spectra of the bottomonium and charmonium states.

Some time ago, there was a breakthrough that drastically improved the predictive power of perturbative QCD for the QCD potential and the heavy quarkonium spectrum: the perturbative predictions for these quantities became much more accurate. This was achieved by properly eliminating contributions from infrared (IR) degrees of freedom in the computations [4,5]. The central quantity is the total energy of a static quark–antiquark pair, defined by the sum of the quark and antiquark pole masses and the QCD potential, $E_{\rm tot}(r) = 2m_{\rm pole} + V_{\rm QCD}(r)$. We can achieve the decoupling of IR degrees of freedom (renormalon cancellation) at each order of the perturbative expansion by
(1) re-expressing the quark pole mass in terms of a so-called short-distance mass, such as the $\overline{\rm MS}$ mass, and
(2) expanding $m_{\rm pole}$ and $V_{\rm QCD}(r)$ in the same coupling constant.[1]

As a result, the perturbative predictions become stable against a variation of the renormalisation scale μ, and also the perturbative series show a much better convergence behaviour, as compared to those in the conventional computations.

It was then natural to compare the perturbative QCD predictions with existing experimental data or with other theoretical predictions which incorporate non-perturbative effects. The main aim of this program is to clarify the differences between the perturbative QCD predictions and the full QCD predictions, given the more accurate predictions of the former. The first comparison [6] was made for the bottomonium spectrum (and also for part of the charmonium spectrum) between the perturbative prediction and the experimental data. It was followed by a comparison [7] between the perturbative QCD prediction of the QCD potential and typical phenomenological potentials (used in phenomenological approaches to heavy quarkonium physics), and then by a comparison [8] of the QCD potential between perturbative QCD predictions and a lattice computation. More elaborated analyses on each of these comparisons followed subsequently [9–13]. In all of these analyses, when IR contributions were appropriately eliminated, the perturbative QCD predictions turned out to agree with the experimental data/phenomenological potentials/lattice results within estimated perturbative uncertainties. Contrary to wide beliefs, there were no indications of large non-perturbative effects. Only much smaller

* From March 2003: Physikdepartment T31, Technische Universität München, 85747 Garching, Germany

[1] This is somewhat involved technically, since usually $m_{\rm pole}$ and $V_{\rm QCD}(r)$ are expressed in terms of different coupling constants

non-perturbative contributions, which can be absorbed into perturbative uncertainties, appear to be compatible with these analyses.

In this paper we are concerned with the third type of comparison: perturbative QCD prediction versus lattice calculations. In the previous comparisons of this type, the leading renormalon uncertainty of the perturbative QCD potential was removed in various manners. In [8], the inter-quark force (improved by renormalisation group methods) was used instead of the QCD potential[2]; in [11], the leading renormalon contribution (estimated by a sophisticated approximation) was subtracted from the QCD potential by hand; in [12], the perturbative series was Borel-resummed, taking into account the leading renormalon pole appropriately. We examine yet another method for removing the leading renormalon. Namely, we examine the total energy $E_{\rm tot}(r)$, as defined above, after re-expressing it in terms of the $\overline{\rm MS}$ mass renormalised at the $\overline{\rm MS}$ mass scale, $\overline{m} \equiv m^{\overline{\rm MS}}(m^{\overline{\rm MS}})$. To achieve stable predictions over a wide range of r, we adopt the scale-fixing prescriptions of [7,10]. These prescriptions introduce the scales dependent on r and $\overline{m}$, $\mu = \mu(r, \overline{m})$, which are consistent with physical expectations.

As stated, $E_{\rm tot}(r)$ constitutes the leading part of the non-relativistic Hamiltonian of the heavy quarkonium system within the potential–NRQCD framework. We may expect that a direct comparison of $E_{\rm tot}(r)$, which determines the bulk of the heavy quarkonium spectrum, would provide a clearer picture of the present status on the credibility of the theoretical predictions based on the potential–NRQCD framework, supplemented either by perturbative QCD computations or by lattice computations of the potentials; see e.g. [13–16] for analyses in this direction. Furthermore, the scale-fixing prescription for $E_{\rm tot}(r)$ we adopt here is the only prescription which has been used in the perturbative QCD predictions for the level structure of the bottomonium states (including higher excited states) incorporating the renormalon cancellation. We will see that indeed this prescription stabilizes the perturbative prediction up to large distances, and hence it is suited for predicting the energy levels of excited states of the heavy quarkonium systems.

According to the renormalon argument, an uncertainty of the perturbative QCD prediction for $E_{\rm tot}(r)$ grows rapidly at large distances as $\Lambda_{\rm QCD}^3\, r^2$ [17]. It is nevertheless important to predict $E_{\rm tot}(r)$ perturbatively at large r for the following reasons.

(1) The level spacings among the bottomonium spectrum have uncertainties smaller than the uncertainties of individual levels. This is because the errors of $E_{\rm tot}(r)$ at different r are generally correlated. Indeed, the estimate of the error of $E_{\rm tot}(r)$, by changing input parameters or scale-fixing prescriptions, is perfectly consistent with $\Lambda_{\rm QCD}^3\, r^2$ [7,10]; on the other hand, the bottomonium level spacings vary less, because the individual levels vary in a correlated way. This is why the perturbative QCD predictions of the whole level structure of the bottomonium in [6,9,13] made sense.

(2) Many physical quantities of heavy quarkonium states are sensitive to the short-distance part of the potential. For instance, the fine splittings of the bottomonium excited states are sensitive to much shorter distance part of $E_{\rm tot}(r)$ as compared to the individual levels. As a result, perturbative uncertainties of the fine splittings are much more suppressed (of order $\Lambda_{\rm QCD}^3/m^2$) as compared to uncertainties of the individual levels which directly reflect uncertainties of $E_{\rm tot}(r)$. Predictability of $E_{\rm tot}(r)$ up to large distances ensures that the wave functions of the excited states can be computed in the computation of the fine splittings [13], although only the short-distance parts of the wave functions are relevant. The order $\Lambda_{\rm QCD}^3\, r^2$ uncertainty of $E_{\rm tot}(r)$ at large distances is just appropriate to ensure the theoretical uncertainties ($\Lambda_{\rm QCD}^3/m^2$) of the fine splittings. These theoretical uncertainties, as well as the level of agreement with the experimental values, of the computed fine splittings (and the hyperfine splittings) turn out to be comparable to those of the recent lattice computations of these splittings; see [13,18] for details.

In our comparison of the QCD potential between perturbative QCD and lattice computations, we benefit from considering a hypothetical world which contains no light quark flavours. It is then possible to use the lattice calculations of the QCD potential in the quenched approximation. On the other hand, in the perturbative prediction for $E_{\rm tot}(r)$, we have an additional parameter. Although naively the quark mass is simply a constant independent of r, due to our specific scale-fixing prescriptions, the value of $\overline{m}$ affects the r-dependence of $E_{\rm tot}(r)$ non-trivially. For a heavy quarkonium system in this hypothetical world, there is no strong motivation to choose a specific value for $\overline{m}$ (as opposed to the studies [7,10]). Therefore, in our analysis, we treat $\overline{m}$ as a controllable parameter for testing stability of the perturbative prediction. We will show that for those choices of $\overline{m}$ that give stable predictions, $E_{\rm tot}(r)$ is independent of $\overline{m}$ up to deviations of the order of the expected theoretical uncertainty (after a suitable shift by an r-independent constant). By varying $\overline{m}$ to achieve optimum convergence for large r, we can obtain perturbative QCD predictions up to fairly long distances and compare them to the results of lattice QCD.

The organisation of this paper is as follows: Sect. 2 sets our conventions and gives some details of our perturbative QCD calculation. Section 3 compares the lattice and perturbative QCD data. Conclusions are given in Sect. 4. We collect formulae related to the renormalisation-group evolution of the strong coupling constant in the appendix.

2 Conventions and framework

We would like to compare the lattice data and the perturbative predictions corresponding to the same theoretical input. This will be carried out in the following manner. For each lattice data set we calculate the Sommer scale r_0

[2] See also [7] for some theoretical discussion on the inter-quark force

defined by

$$r^2 \left.\frac{\mathrm{d}V_{\mathrm{QCD}}}{\mathrm{d}r}\right|_{r=r_0} = 1.65. \tag{1}$$

Then the lattice data are expressed in units of r_0. The perturbative computations are expressed in terms of the strong coupling constant defined in the theory with $n_l = 0$ active flavours. We convert all the results into units of r_0 using the relation between the Lambda parameter of the running coupling constant (in the $\overline{\mathrm{MS}}$ scheme) and the Sommer scale [19]: $\Lambda_{\overline{\mathrm{MS}}} = 0.602(48)\, r_0^{-1}$. We use the central value of this relation in the main part of our analysis; the effect of a variation of $\Lambda_{\overline{\mathrm{MS}}}$ inside the error interval is discussed at the end of Sect. 3. All the predictions are compared in units of r_0. Furthermore, in order to maintain physical intuition, we will also use physical units. Although there exists no rigid correspondence between the physical scales of the real world and of the hypothetical world, we follow the convention of the lattice calculations in the quenched approximation. The numerical value on the right-hand-side of (1) has been chosen so that for phenomenological potentials $r_0 \approx (400\,\mathrm{MeV})^{-1}$. Whenever we refer to values in units of MeV or GeV, we invoke this translation.

The total energy of a static quark–antiquark system is given by

$$E_{\mathrm{tot}}(r) = 2m_{\mathrm{pole}} + V_{\mathrm{QCD}}(r)\,. \tag{2}$$

In perturbative QCD, the pole mass m_{pole} is related to the $\overline{\mathrm{MS}}$ mass $\overline{m}$ up to three loops by the relation

$$m_{\mathrm{pole}} = \overline{m}\left\{1 + \frac{4}{3}\frac{\alpha_{\mathrm{S}}(\overline{m})}{\pi} + \left(\frac{\alpha_{\mathrm{S}}(\overline{m})}{\pi}\right)^2 d_1 + \left(\frac{\alpha_{\mathrm{S}}(\overline{m})}{\pi}\right)^3 d_2\right\}. \tag{3}$$

The QCD potential up to $\mathcal{O}(\alpha_{\mathrm{S}}^3)$ is given by

$$V_{\mathrm{QCD}}(r) = -\frac{4}{3}\frac{\alpha_{\mathrm{S}}(\mu)}{r}\left[1 + \left(\frac{\alpha_{\mathrm{S}}(\mu)}{4\pi}\right)(2\beta_0\ell + a_1) + \left(\frac{\alpha_{\mathrm{S}}(\mu)}{4\pi}\right)^2\left\{\beta_0^2\left(4\ell^2 + \frac{\pi^2}{3}\right) + 2(\beta_1 + 2\beta_0 a_1)\ell + a_2\right\}\right], \tag{4}$$

where $\ell = \log(\mu r) + \gamma_{\mathrm{E}}$.

Here and hereafter, we have set the number of light flavours, n_l, to zero, i.e. we will be neglecting the effects of light quark loops. This corresponds to the quenched approximation in lattice QCD to which we want to compare the perturbative results. The running coupling $\alpha_{\mathrm{S}}(\mu)$ depends on n_l through the coefficients of the beta function; the constants d_1, d_2, a_1 and a_2 also get contributions from light quark loops and therefore depend on n_l. For $n_l = 0$, their values are $\beta_0 = 11$, $\beta_1 = 102$, $d_1 \approx 13.443$, $d_2 \approx 190.39$, $a_1 = 31/3$ and $a_2 \approx 456.74$. The analytical formulae can be found in [10].[3]

[3] These formulae have originally been computed in [20, 21]. The mass relation (3) is re-expressed in terms of the coupling of the theory without heavy quarks

After re-expressing $\alpha_{\mathrm{S}}(\overline{m})$ in (3) in terms of $\alpha_{\mathrm{S}}(\mu)$ by using the running of α_{S} [see (8) in the appendix], and dropping terms of $\mathcal{O}(\alpha_{\mathrm{S}}(\mu)^4)$ and higher, we obtain the total energy $E_{\mathrm{tot}}(r; \overline{m}, \alpha_{\mathrm{S}}(\mu), \mu)$ which does not suffer from the leading renormalon uncertainty.

Due to the truncation of the perturbative series at finite order, E_{tot} depends on the renormalisation scale μ. Two scale-fixing prescriptions have been introduced in [7].

(1) The scale $\mu = \mu_1(r)$ is fixed by demanding stability of $E_{\mathrm{tot}}(r)$ against variation of the scale:

$$\mu\frac{\mathrm{d}}{\mathrm{d}\mu}E_{\mathrm{tot}}(r; \overline{m}, \alpha_{\mathrm{S}}(\mu), \mu)\Big|_{\mu=\mu_1(r)} = 0. \tag{5}$$

(2) The scale $\mu = \mu_2(r)$ is fixed to the minimum of the absolute value of the last known term [$\mathcal{O}(\alpha_{\mathrm{S}}^3)$ term] of $E_{\mathrm{tot}}(r)$:

$$\mu\frac{\mathrm{d}}{\mathrm{d}\mu}\left[E_{\mathrm{tot}}^{(3)}(r; \overline{m}, \alpha_{\mathrm{S}}(\mu), \mu)\right]^2\Big|_{\mu=\mu_2(r)} = 0. \tag{6}$$

Although these prescriptions are very different, it has been shown that where both prescriptions exist, the total energy is virtually identical for both prescriptions. As a general feature of $E_{\mathrm{tot}}(r)$, the convergence of the perturbative series improves and the scale dependence decreases, if we choose larger μ for smaller distances and smaller μ for larger distances. Consequently, the range of the perturbative calculation can be extended to much larger r with these prescriptions than what would be possible with a fixed, r-independent scale.

The prescriptions for the renormalon cancellation and the scale fixing we adopt here follow (basically) those in [7, 10, 13]. We refer the reader to these papers for more detailed features of the perturbative predictions in these prescriptions.

There are several methods to assess the reliability of the prediction at a given distance: e.g. one can compare the total energies as determined with the scales from both prescriptions, one can compare the sizes of the individual terms of the perturbative expansion of E_{tot} or one can study the scale dependence of E_{tot} around the respective scale. We will use these methods in Sect. 3.

The convergence properties of $E_{\mathrm{tot}}(r)$ strongly depend on the mass parameter $\overline{m}$. We illustrate this in Table 1 for $r = 2r_0 \simeq 5\,\mathrm{GeV}^{-1}$. $E_{\mathrm{tot}}^{(i)}$ denotes the $\mathcal{O}(\alpha_{\mathrm{S}}^i)$ term of the perturbative series of E_{tot}. It can be seen that the series converges nicely, especially for $\overline{m} \simeq 3\,\mathrm{GeV}$. In Sect. 3 we will see that those values for $\overline{m}$ that provide best convergence also provide an optimal agreement with lattice results. We find that, to our surprise, the perturbative series converges for distances as large as $3r_0 \simeq 7.5\,\mathrm{GeV}^{-1}$. (Generally, the convergence behaviour of $E_{\mathrm{tot}}(r)$ becomes worse for larger r.) We note that the values of the scales $\mu_{1,2}$ stay much larger than $1/r$. See [7] for discussion on this aspect.

For large distances, E_{tot} depends on whether we use the analytical solution or numerical solution of the renormalisation-group equation for the running of the strong

Table 1. Convergence properties of $E_{\rm tot}$ for $r = 2r_0 \simeq 5\,\mathrm{GeV}^{-1}$. All numbers in GeV

$\overline{m}$	$\mu = \mu_1$					$\mu = \mu_2$				
	μ	$E_{\rm tot}^{(1)}$	$E_{\rm tot}^{(2)}$	$E_{\rm tot}^{(3)}$	$E_{\rm tot}$	μ	$E_{\rm tot}^{(1)}$	$E_{\rm tot}^{(2)}$	$E_{\rm tot}^{(3)}$	$E_{\rm tot}$
1.6	0.389	1.275	0.271	−0.280	4.466	0.419	0.921	0.243	0	4.364
1.8	0.413	1.126	0.109	−0.147	4.687	0.449	0.881	0.158	0	4.639
2.0	0.436	1.08	0.038	−0.096	5.022	0.477	0.882	0.111	0	4.993
2.2	0.458	1.073	−0.007	−0.069	5.397	0.502	0.901	0.077	0	5.378
2.4	0.478	1.085	−0.042	−0.051	5.792	0.525	0.929	0.049	0	5.778
2.6	0.497	1.109	−0.072	−0.039	6.197	0.545	0.965	0.022	0	6.187
2.8	0.515	1.140	−0.102	−0.029	6.609	0.563	1.006	−0.005	0	6.601
3.0	0.530	1.179	−0.133	−0.021	7.025	0.576	1.055	−0.035	0	7.019
3.2	0.543	1.224	−0.168	−0.012	7.444	0.453	1.680	−0.682	0	7.398
3.4	0.553	1.277	−0.208	−0.004	7.865	0.507	1.451	−0.393	0	7.859
3.6	0.559	1.342	−0.262	0.006	8.287	0.577	1.288	−0.207	0.005	8.287
3.8	0.554	1.439	−0.352	0.023	8.711	0.615	1.268	−0.173	0.012	8.708

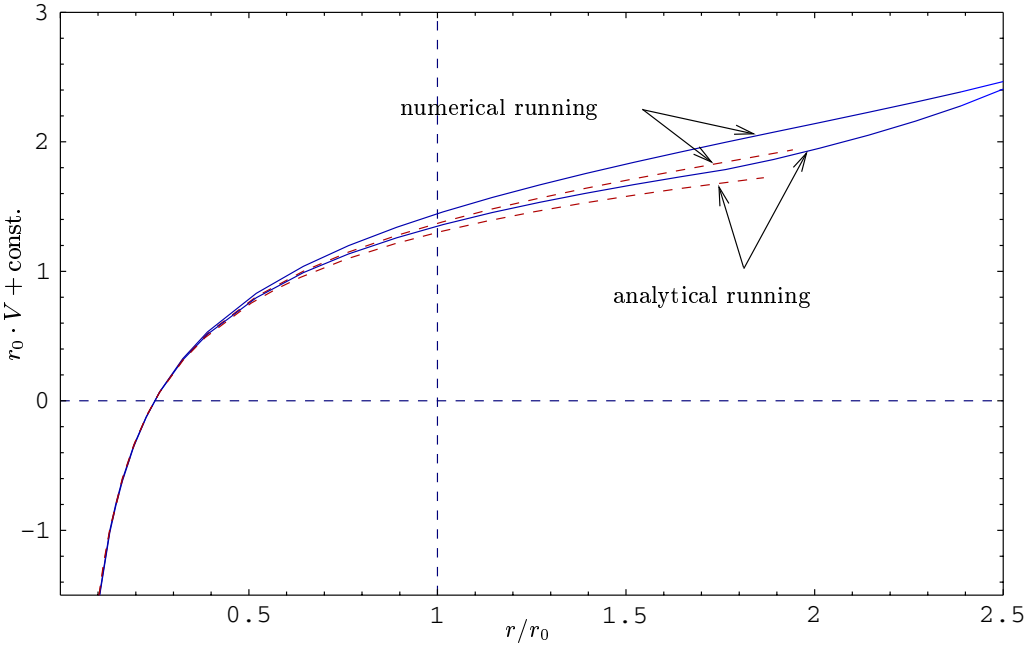

Fig. 1. Comparison between analytical and numerical running. The solid lines correspond to $\overline{m} = 3\,\mathrm{GeV} \simeq 7.5/r_0$, the dashed ones to $\overline{m} = 4\,\mathrm{GeV} \simeq 10/r_0$

coupling constant $\alpha_{\rm S}(\mu)$ (see the appendix). We show the total energy for both types of running in Fig. 1 for two values of $\overline{m}$. In accordance with our previous works [7, 10] we employ the numerical solution of the renormalisation-group equation below. Our results do not change qualitatively if we use the analytical running instead.

To end this section, we briefly summarise the argument on the renormalons included in $E_{\rm tot}(r)$.

(1) After the $\mathcal{O}(\Lambda_{\rm QCD})$ renormalon is cancelled, the perturbative series of $E_{\rm tot}(r)$ is estimated to have the following behaviour. The $\mathcal{O}(\alpha_{\rm S}^{n+1})$ term of the series expansion of $E_{\rm tot}(r)$ behaves as const. $\times\, r^2\, n!\, (\beta_0\alpha_{\rm S}/(6\pi))^n\, n^{3\delta/2}$ for $n \gg 1$, where $\delta = \beta_1/\beta_0^2$. Because of the factorial $n!$, the series is only an asymptotic series, namely it diverges for large enough n. Hence, there is a limitation to the achievable accuracy of the perturbative prediction for $E_{\rm tot}(r)$. It can be estimated from the size of the terms around the minimum, $n \approx 6\pi/(\beta_0\alpha_{\rm S})$; this gives an uncertainty of order $\Lambda_{\rm QCD}^3 r^2$. The behaviour of the series depends on the value of the expanding parameter $\alpha_{\rm S} \equiv \alpha_{\rm S}(\mu)$, or equivalently, on the choice of the scale μ. The uncertainty, $\Lambda_{\rm QCD}^3 r^2$, is independent of $\alpha_{\rm S}(\mu)$ or μ, nonetheless. (For details, see [22, 23].)

(2) Based on the above argument, we may optimise convergence of the series by appropriately choosing the scale μ. In this case, even with the series expansion up to $\mathcal{O}(\alpha_{\rm S}^3)$ we may estimate the uncertainty of $E_{\rm tot}(r)$ to be of order $\Lambda_{\rm QCD}^3 r^2$ from the size of the truncated next-order term or

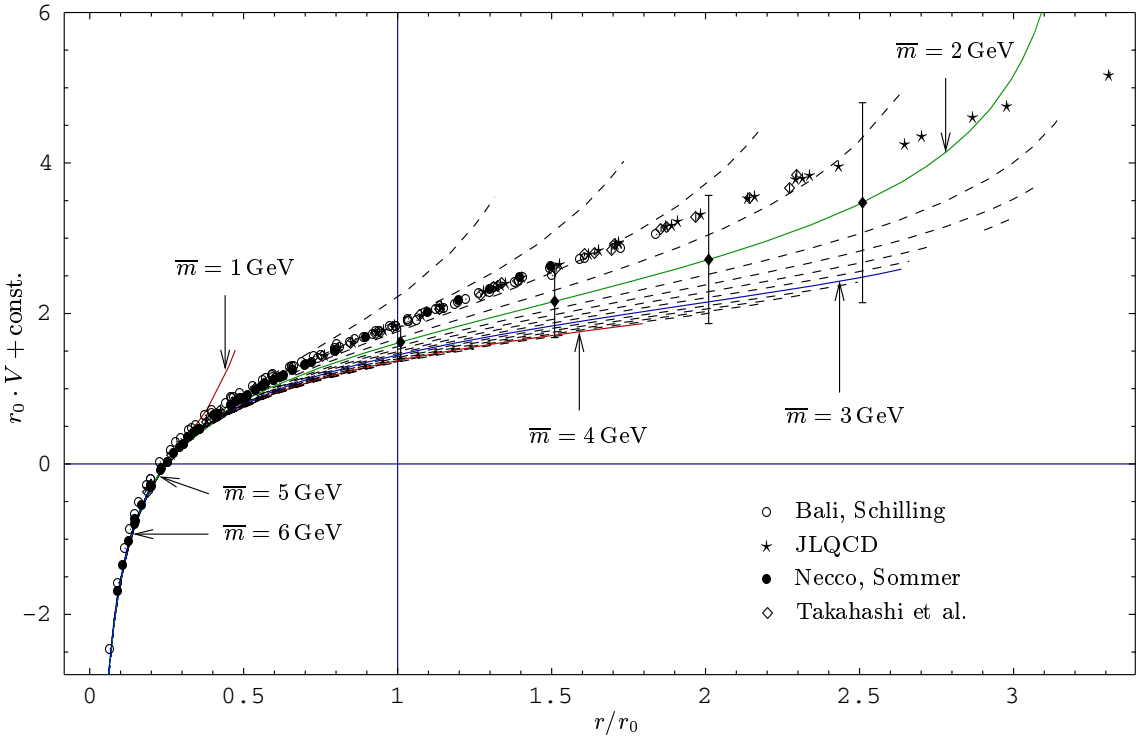

Fig. 2. Comparison between perturbative and lattice calculations of the QCD potential. The lines correspond to masses between 1 and 6 GeV in steps of 0.2 GeV (solid lines for integer masses, $1\,\mathrm{GeV} \simeq 2.5/r_0$, the lines for $\overline{m} \gtrsim 4\,\mathrm{GeV}$ are masked by the other lines). The points correspond to Bali/Schilling (○) [24], Takahashi et al. (◇) [25], JLQCD (⋆) [26] and Necco/Sommer (●) [27]. Error bars for the statistical errors of the lattice data are plotted where given by the authors, but they are generally smaller than the size of the symbols. Lines are plotted only when the total energies determined by the two prescriptions differ by less than $0.5/r_0$

from the scale dependence of $E_{\mathrm{tot}}(r)$ around the optimised scale. Indeed, explicit numerical examinations of $E_{\mathrm{tot}}(r)$ up to $\mathcal{O}(\alpha_{\mathrm{S}}^3)$ support this argument [7,8,10,11].
(3) One may factorise the infrared part of $E_{\mathrm{tot}}(r)$ using an operator product expansion [2]. In this way, one may absorb the order $\Lambda_{\mathrm{QCD}}^3 r^2$ renormalon into a matrix element of an operator, while defining a Wilson coefficient perturbatively that is free from the renormalon and dependent on the factorisation scale. More generally, one may separate $E_{\mathrm{tot}}(r)$ into perturbative coefficients free from renormalons and non-perturbative parameters (matrix elements) including renormalons. (This factorisation is beyond the scope of the present paper.)

3 Comparison of perturbative and lattice calculations

For comparison with the perturbative predictions of the QCD potential as explained in the previous section, four different sets of lattice data calculated in the quenched approximation are used: those from [24] ($\beta = 6.8$), from [25] ($\beta = 6.0$), from [26] ($\beta = 6.0$) and from [27] ($6.57 \leq \beta \leq 6.92$). All the lattice data have been corrected using the lattice Coulomb potential to match the continuum definition of the QCD potential at short distances.

For comparison of the perturbative and the lattice data, we have to account for an r-independent additive constant that is not determined by lattice calculations. Since perturbative calculations are more reliable at small distances and lattice calculations are more reliable at larger distances, we adopt the following procedure: the different sets of lattice data are converted to physical units with the lattice spacing as given by the authors of the respective papers, or (where the lattice spacing was not explicitly derived) by fixing the Sommer scale with the phenomenological potential fit as performed by the authors of the respective papers. Then we adjust the sets of lattice data among each other to make them coincide at $r = r_0$ by adding constants. Finally we shift both the perturbative and the lattice data so that they vanish at $r = r_0/4$, where in the case of the lattice results the data from [27] is used.

We see that the sets of lattice data [24–27] corresponding to different values of β are located almost on the same curve (Fig. 2). This shows that the dependence of the lattice results on the lattice spacing is negligibly small, i.e. discretization errors in the lattice calculations are negligible in our comparison.

As described before, the perturbative calculation has two input parameters, these can be e.g. $\Lambda_{\overline{\mathrm{MS}}}$ and $\overline{m}$. The potential depends on the mass $\overline{m}$ (after shifting to E_{tot} $(r_0/4) = 0$) only through the $\log(\overline{m}/\mu)$-terms in the relation between the pole mass and the $\overline{\mathrm{MS}}$ mass. We find that

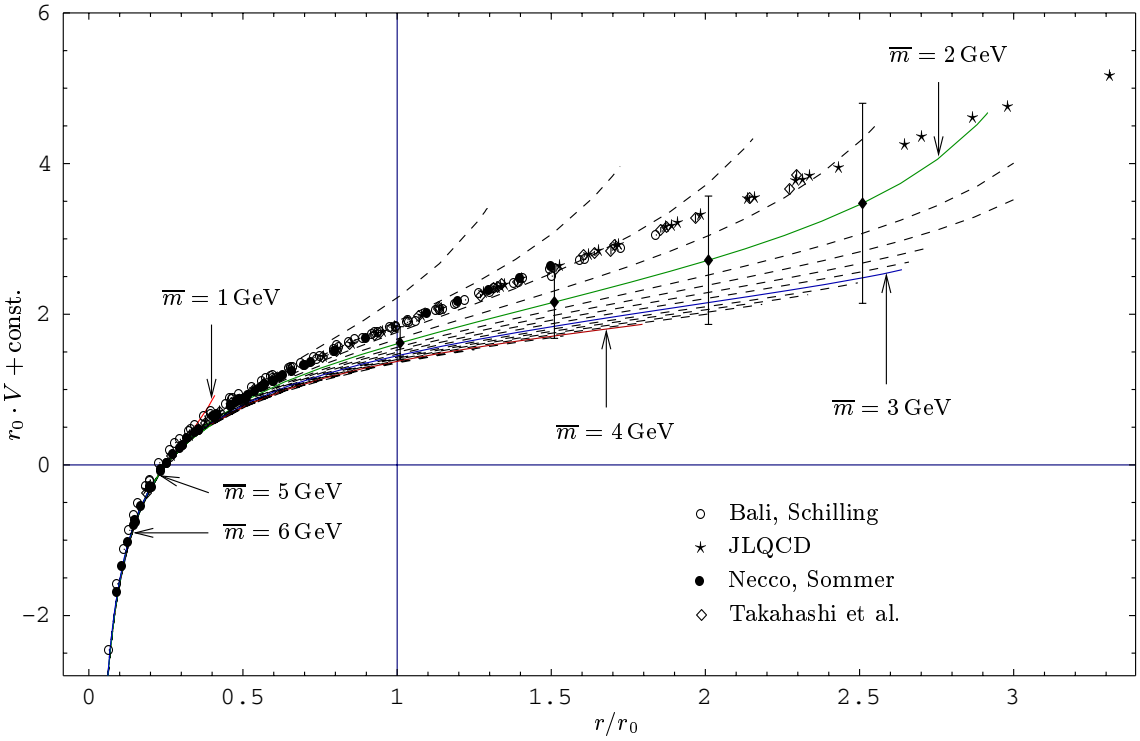

Fig. 3. Comparison between perturbative and lattice calculations of the QCD potential. The lines correspond to masses between 1 and 6 GeV in steps of 0.2 GeV. Lines are plotted only when a +10% scale change makes the total energy vary by less than 20%

(after shifting the curves to make them coincide at $r_0/4$), for small distances $r < r_0/4$ the curves are identical, for larger distances the curves corresponding to different $\overline{m}$ start to differ from each other. The quality of convergence and the stability against scale changes varies strongly with $\overline{m}$.

In Fig. 2 we plot the QCD potential for various values of $\overline{m}$ between 1 and 6 GeV in steps of 0.2 GeV. To ensure that only reasonably stable and reliable predictions are shown, the curves are drawn only in those points, where the energies as determined by the two different scale-fixing prescriptions differ by less than $0.5/r_0$. We find that the resulting curves span a band around the lattice data that increases in width with increasing r. The width of this band is consistent with the expected theoretical uncertainty due to the uncancelled next-to-leading renormalon [17], $\pm\frac{1}{2}\Lambda^3 r^2$, with $\Lambda = 300\,\mathrm{MeV}$, indicated by the error bars in the figure. We find a very good agreement between the lattice results and the curves that show the largest range of convergence, but even for those choices of $\overline{m}$ where the prediction becomes unstable earlier, the agreement is still good.

To show that the good agreement between the perturbative and the lattice calculations does not depend on a specific stability criterion, in Fig. 3 we show the same comparison as in Fig. 2, but this time we do not consider the difference between the energies as determined with the two different scale prescriptions, but the stability against scale change. We plot the curves only in those points where a scale change of +10% makes the total energy vary by less than ±20%.

We would like to stress that we do not tune the mass parameter to achieve good agreement with the lattice results, but we vary it to find those values of $\overline{m}$ that give optimal convergence of the perturbative series. It can be seen in the figures that the curves for those values of $\overline{m}$ that have the largest range of convergence, the agreement with the lattice data is close to optimal.

We now compare our results to those of [11]. In that paper, a fixed, r-independent scale μ is used for the perturbative QCD potential. We find that our formalism almost exactly reproduces the curves of [11] for large values of $\overline{m}$ (Fig. 4). The explanation for this behaviour is the following. While in our formalism the scale is strongly dependent on r even for large masses (see Fig. 5), the scale tends to rise with $\overline{m}$. For $\overline{m} \sim 3\,\mathrm{GeV}$ the r-dependent scale varies around 1 GeV, for $\overline{m} \sim 10\,\mathrm{GeV}$ it varies around 3 GeV. Independent of $\overline{m}$, however, the scale dependence of E_{tot} is strong for scales around 1 GeV and very weak for scales around 3 GeV (Fig. 6); therefore, choosing a large $\overline{m}$ in our formalism gives a result very close to the treatment of [11]. We can also see that for these large masses our stability criteria indicate a range of convergence up to about $r_0/2$. Our analysis is therefore consistent with that of [11], and the results of the latter are reproduced with our formalism by choosing large values for $\overline{m}$.

The perturbative predictions which are most stable at long distances in Figs. 2 and 3 ($\overline{m} \sim$ 2–3 GeV) turn out to be less steep than the lattice data at $r/r_0 \gtrsim 0.5$.

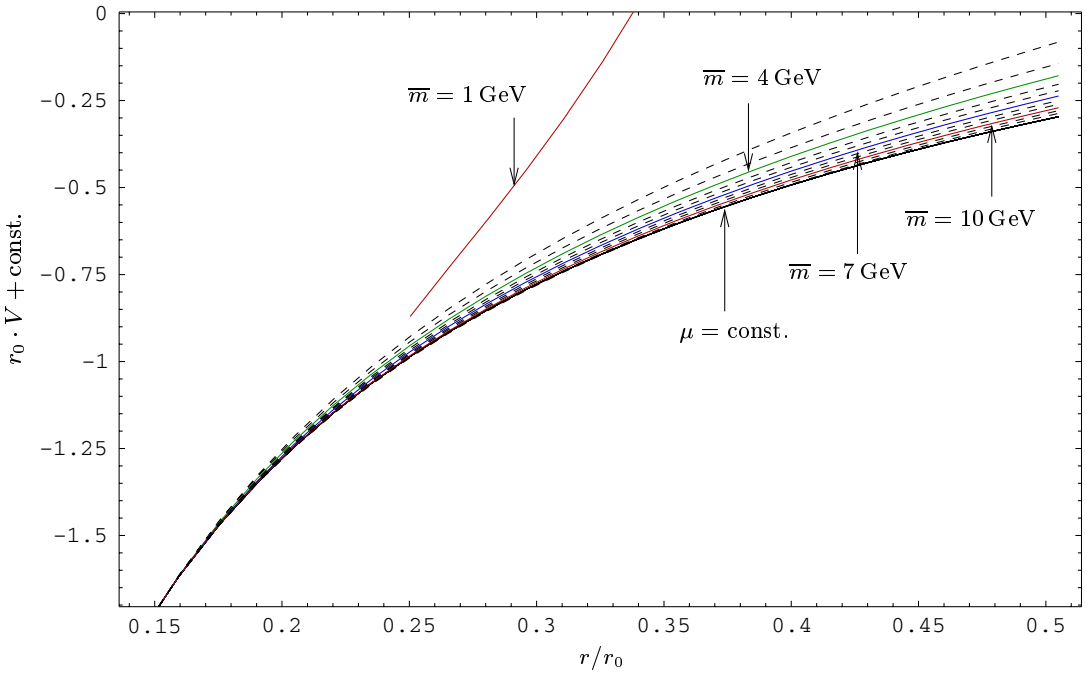

Fig. 4. Comparison between our formalism and the 2-loop QCD potential according to the formalism of [11]. The lowermost line shows the ($\overline{m}$ independent) potential for a constant $\mu = (0.15399\, r_0)^{-1}$, corresponding to the formalism of [11]. The other lines show our results for masses from 1 to 12 GeV in steps of 1 GeV (solid lines for 1, 4, 7 and 10 GeV)

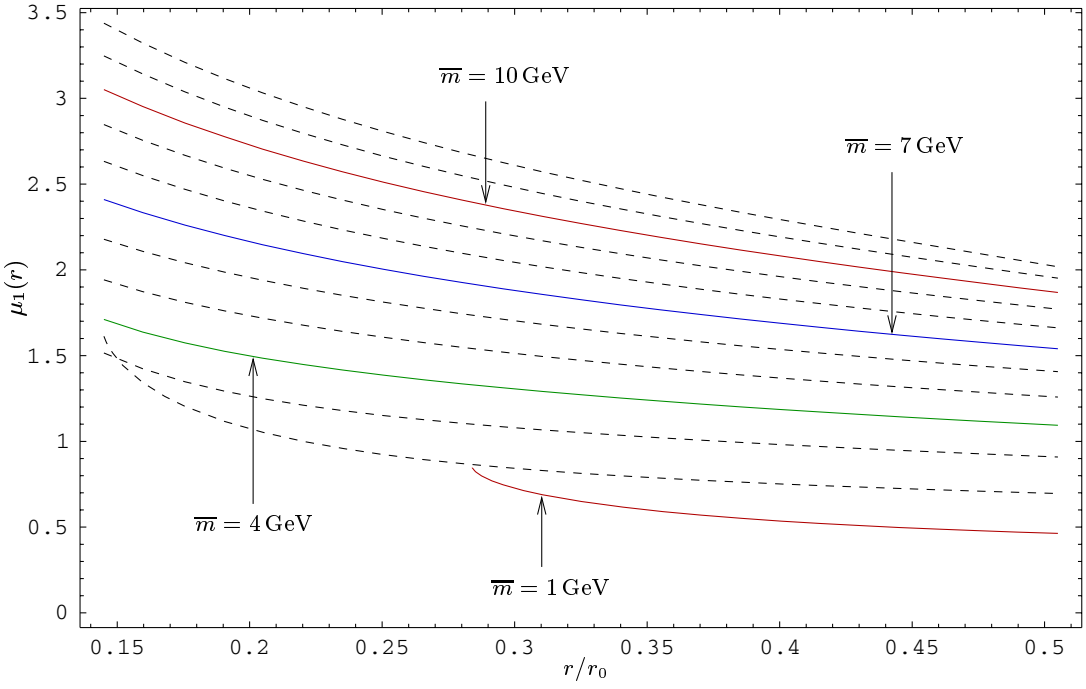

Fig. 5. Scales as determined by the first prescription (5) for values of $\overline{m}$ between 1 and 12 GeV

Qualitatively, we expect that the larger the strong coupling constant the steeper the potential, because the interquark force becomes stronger [7]. This behaviour can be seen in Fig. 7 where we have varied $\Lambda_{\overline{\mathrm{MS}}}\, r_0$ in the interval given in [19], $\Lambda_{\overline{\mathrm{MS}}} = (0.602 \pm 0.048)\, r_0^{-1}$. The lower bound, centre and upper bound of this interval correspond to $\alpha_{\mathrm{S}}^{n_l=0}(M_Z) = 0.0801$, 0.0811 and 0.08205, respectively. The larger value for $\Lambda_{\overline{\mathrm{MS}}}$ (if $r_0 \approx 2.5$ GeV^{-1} is fixed) results in a slightly steeper curve that reproduces the slope of the lattice data better than the central value.

We would like to make two comments in this context. (i) We compared the perturbative QCD potential (including effects of light quark loops) with phenomenological potentials in [10]. There, the perturbative prediction with the

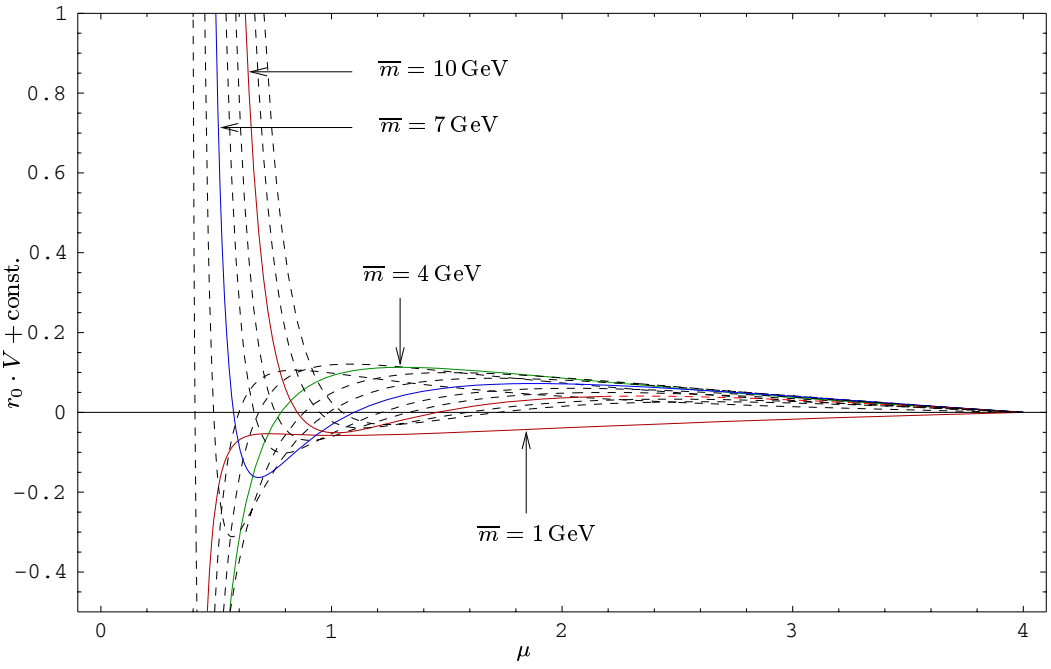

Fig. 6. Dependence of $E_{\mathrm{tot}}(r = 0.3\,r_0)$ on the scale μ for values of $\overline{m}$ between 1 and 15 GeV. Independent of $\overline{m}$, the scale dependence is strong for $\mu \lesssim 1\,\mathrm{GeV}$ and weak for $\mu \gtrsim 1\,\mathrm{GeV}$

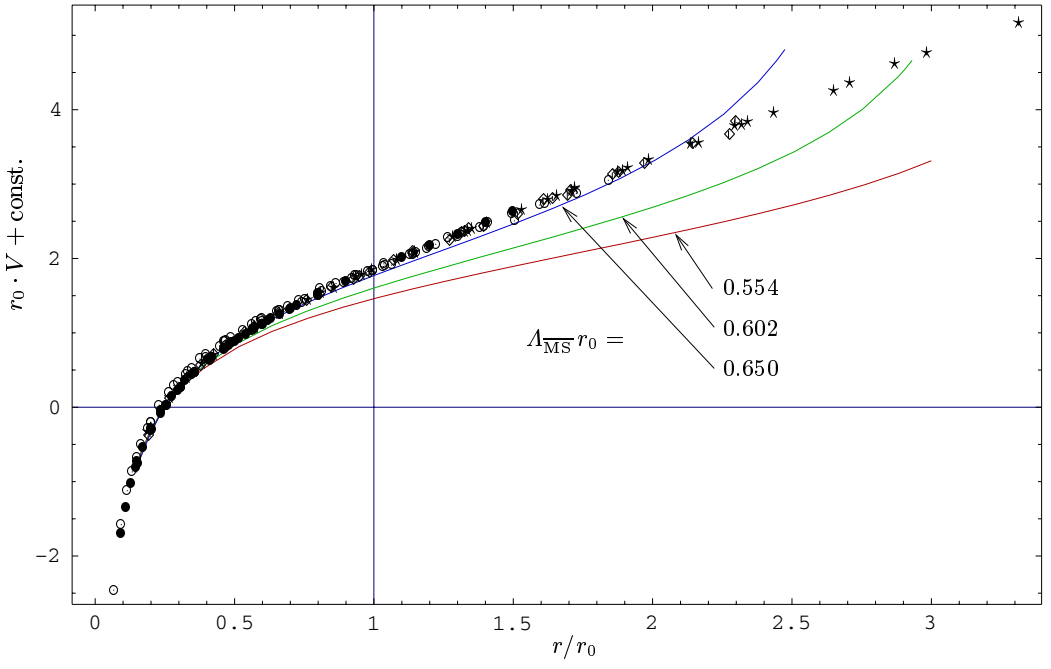

Fig. 7. Dependence of the perturbative results on $\Lambda_{\overline{\mathrm{MS}}} r_0$, the curves shown correspond to the centre and upper and lower bounds of the error interval given in [19]. The middle curve corresponds to the one in Fig. 3 that has the error bars attached to it ($\overline{m} = 2\,\mathrm{GeV}$)

input $\alpha_{\mathrm{S}}(M_Z) = 0.1181$ (the present central value) turned out also to be slightly less steep than the phenomenological potentials at long distances. As a result, a somewhat larger coupling $\alpha_{\mathrm{S}}(M_Z) = 0.1191$–$0.1201$ was favoured for a better agreement with the phenomenological potentials. (ii) In [11], the $\mathcal{O}(\alpha_{\mathrm{S}}^4)$ correction to the perturbative QCD potential (including the ultrasoft effects) was estimated and included in a comparison with the lattice data. The estimated correction makes the potential somewhat steeper. This is consistent with a naive expectation that such an effect is caused by an acceleration of the running of the coupling constant due to the 4-loop coefficient of the beta function. Thus, agreement of the perturbative potential with the lattice data may become even better than our

present analysis when the full next-order correction is calculated and included in the future. Furthermore, we have confirmed that the agreement between the perturbative and lattice data becomes even better if we use the 4-loop running of the coupling constant.

4 Conclusions

We have compared perturbative QCD and lattice QCD predictions for the QCD potential. We examined the perturbative QCD prediction for $E_{\rm tot}(r) = 2m_{\rm pole} + V_{\rm QCD}(r)$, taking specific prescriptions for fixing the renormalisation scale μ. We find that, by adjusting the mass parameter $\overline{m}$, the perturbative prediction can be made stable up to distances $r \sim 3\,r_0$. Whenever we obtain stable perturbative predictions, they agree with the lattice data within the uncertainty estimated from the residual renormalon of order $\Lambda^3 r^2$. We emphasise that we do not tune $\overline{m}$ to fit the lattice data, but we tune $\overline{m}$ to achieve stability of the perturbative prediction, and then the agreement follows. Comparisons of perturbative QCD predictions and lattice data have been performed before, e.g. in [11,12], but only up to distances of $0.5\,r_0$ and $0.9\,r_0$, respectively. If we take an optimal value of $\overline{m}$, our prescriptions for the perturbative prediction of the QCD potential seem to give stable predictions to furthest distances among those examined so far.

Our analysis provides a firmer ground to the analyses of [6,9,13], which predicted the bottomonium energy levels up to the $n = 3$ states using (essentially) the same scale-fixing prescriptions as in the present analysis.[4] We note that the same conclusion could not be drawn directly from the previous comparisons [8,11,12] between the lattice and perturbative computations of the QCD potential, because the prescriptions adopted in those analyses have never been used in perturbative computations of the heavy quarkonium level structure including higher excited states. In the light of our present result, the scale-fixing prescription adopted here is optimal for stable predictions for the energy levels of excited states. Our result supports the estimates of theoretical uncertainties by the next-to-leading renormalon made in [6,9,13].

Whenever stable perturbative predictions are obtained, all the perturbative predictions with different prescriptions for subtracting the leading renormalon agree with one another and also with the lattice data, within the estimated uncertainty. In particular, our perturbative predictions for large $\overline{m}$ reproduce the $\mathcal{O}(\alpha_{\rm S}^3)$ perturbative prediction of [11]. The fact that the different prescriptions have led to mutually consistent perturbative predictions of the QCD potential, endorses the consistency of the perturbative analyses. The comparisons between the perturbative and lattice data, together with other types of comparisons, provide evidence to the hypothesis that the perturbative prediction agrees with full QCD within the order $\Lambda^3 r^2$ uncertainty. In particular, we consider the independent examinations corresponding to the physical reality ($n_l = 4$ with the non-zero charm quark mass [10]) and to the hypothetical case ($n_l = 0$) to be non-trivial cross checks with respect to the validity of the hypothesis. We may further make non-trivial tests of the hypothesis by varying the number of quark flavours and even the gauge group in comparing the perturbative and lattice calculations.

It is quite surprising that the perturbative calculations turn out to give stable predictions up to such long distances [$3r_0 \approx (130\,{\rm MeV})^{-1}$]. At the present stage the reason is unclear. Although we do not know a clear-cut criterion at which distance a perturbative QCD prediction should break down, possible arguments may be as follows. One point is that the relevant scale μ for $E_{\rm tot}(r)$ is not equal to $1/r$ but considerably larger. Another point that may be worth noting is that the system under consideration would be optimally suited for perturbative QCD computations. It is a colour singlet system having a localised spatial extent, so that we may expect the decoupling of IR degrees of freedom to be realised in a most natural way.[5]

Acknowledgements. We are grateful to T. Kaneko, S. Necco and H. Suganuma for providing the lattice data and to A. Pineda and S. Necco for discussions. S.R. was supported by the Japan Society for the Promotion of Science (JSPS).

Appendix

In this paper we expand the perturbative series of the QCD potential and the quark pole mass in the strong coupling constant defined in the $\overline{\rm MS}$ scheme. The coupling constant obeys the renormalisation-group equation:

$$\mu^2 \frac{\rm d}{{\rm d}\mu^2}\,\alpha_s(\mu) = \beta(\alpha_{\rm S}(\mu)) = -\,\alpha_{\rm S}(\mu) \sum_{n=0}^{\infty} \beta_n \left(\frac{\alpha_{\rm S}(\mu)}{4\pi}\right)^{n+1} . \quad (7)$$

We include the coefficients of the beta function up to 3 loops in our analysis[6], i.e. $\beta_0 = 11$, $\beta_1 = 102$, $\beta_2 = 2857/2$ ($n_l = 0$), and $\beta_n = 0$ for $n \geq 3$.

In rewriting $\alpha_{\rm S}(\overline{m})$ in terms of $\alpha_{\rm S}(\mu)$ in the fixed-order expression of $E_{\rm tot}(r)$, we use the perturbative solution of (7):

$$\alpha_{\rm S}(\overline{m}) = \alpha_{\rm S}(\mu)\left[1 + \frac{\alpha_{\rm S}(\mu)}{\pi}\frac{\beta_0}{2}\log\left(\frac{\mu}{\overline{m}}\right) \right. \quad (8)$$

[4] The value of $\overline{m}$, which stabilizes the perturbative predictions for $E_{\rm tot}(r)$ up to the furthest distance, lies between the bottom and charm quark masses. In this sense, we are in a lucky situation in the predictions of the charmonium and bottomonium spectra

[5] It may be contrasted with e.g. perturbative QCD calculations of parton scattering amplitudes, where spatially separated coloured partons exist as asymptotic states

[6] Although the 4-loop coefficient is available, we consider the use of the 3-loop beta function to be more consistent with the analysis of the fixed-order perturbative series up to $\mathcal{O}(\alpha_{\rm S}^3)$

$$+\left(\frac{\alpha_{\rm S}(\mu)}{\pi}\right)^2\left\{\frac{\beta_0^2}{4}\log^2\left(\frac{\mu}{\overline{m}}\right)+\frac{\beta_1}{8}\log\left(\frac{\mu}{\overline{m}}\right)\right\}+\ldots\Bigg].$$

This relation is inserted to (3) and the series expansion is truncated at order $\alpha_{\rm S}(\mu)^3$. Then $E_{\rm tot}(r)$ is given as a function of r, $\overline{m}$, μ and $\alpha_{\rm S}(\mu)$.

The value of $\alpha_{\rm S}(\mu)$ is determined by the renormalisation-group evolution from the input Lambda parameter defined in the $\overline{\rm MS}$ scheme, $\Lambda_{\overline{\rm MS}}$; see e.g. [28] for the definition of $\Lambda_{\overline{\rm MS}}$. The renormalisation-group evolution of $\alpha_{\rm S}(\mu)$ is calculated in two different ways in this paper. When we refer to "numerical running", we solve the renormalisation-group equation (7) numerically. In this case, $\Lambda_{\overline{\rm MS}} = 0.65573\cdots\times\mu_{\rm Landau}$ ($n_l=0$), where $\mu_{\rm Landau}$ is the position of the infrared singularity (Landau singularity) of the running coupling constant $\alpha_{\rm S}(\mu)$. On the other hand, when we refer to "analytical running", we use an approximate analytic solution of the renormalisation-group equation:

$$\frac{\alpha_{\rm S}(\mu)}{\pi}\approx\frac{4}{\beta_0 L}-\frac{\beta_1\log L}{(\beta_0 L)^2}+\frac{1}{(\beta_0 L)^3}\left[\frac{\beta_1^2}{4}\left(\log^2 L-\log L-1\right)+\beta_2\right], \tag{9}$$

where $L=\log(\mu^2/\Lambda^2_{\overline{\rm MS}})$ and terms of $\mathcal{O}(1/L^4)$ have been neglected.

References

1. A. Pineda, J. Soto, Nucl. Phys. Proc. Suppl. **64**, 428 (1998)
2. N. Brambilla, A. Pineda, J. Soto, A. Vairo, Nucl. Phys. B **566**, 275 (2000)
3. B.A. Kniehl, A.A. Penin, V.A. Smirnov, M. Steinhauser, Nucl. Phys. B **635**, 357 (2002)
4. A. Hoang, M. Smith, T. Stelzer, S. Willenbrock, Phys. Rev. D **59**, 114014 (1999)
5. M. Beneke, Phys. Lett. B **434**, 115 (1998)
6. N. Brambilla, Y. Sumino, A. Vairo, Phys. Lett. B **513**, 381 (2001)
7. Y. Sumino, Phys. Rev. D **65**, 054003 (2002)
8. S. Necco, R. Sommer, Phys. Lett. B **523**, 135 (2001)
9. N. Brambilla, Y. Sumino, A. Vairo, Phys. Rev. D **65**, 034001 (2002)
10. S. Recksiegel, Y. Sumino, Phys. Rev. D **65**, 054018 (2002)
11. A. Pineda, J. Phys. G **29**, 371 (2003)
12. T. Lee, Phys. Rev. D **67**, 014020 (2003)
13. S. Recksiegel, Y. Sumino, Phys. Rev. D **67**, 014004 (2003)
14. N. Brambilla, hep-ph/0012211
15. G. Bali, Phys. Rept. **343**, 1 (2001)
16. N. Brambilla, D. Gromes, A. Vairo, Phys. Rev. D **64**, 076010 (2001)
17. U. Aglietti, Z. Ligeti, Phys. Lett. B **364**, 75 (1995)
18. S. Recksiegel, Y. Sumino, hep-ph/0305178
19. S. Capitani, M. Lüscher, R. Sommer, H. Wittig [ALPHA Collaboration], Nucl. Phys. B **544**, 669 (1999); Erratum **582**, 762 (2000)
20. M. Peter, Phys. Rev. Lett. **78**, 602 (1997); Nucl. Phys. B **501**, 471 (1997); Y. Schröder, Phys. Lett. B **447**, 321 (1999)
21. K. Melnikov, T. v. Ritbergen, Phys. Lett. B **482**, 99 (2000)
22. M. Beneke, Phys. Rept. **317**, 1 (1999)
23. Y. Sumino, hep-ph/0004087
24. G.S. Bali, K. Schilling, Phys. Rev. D **47**, 661 (1993)
25. T.T. Takahashi et al., Phys. Rev. D **65**, 114509 (2002)
26. JLQCD Collaboration, S. Aoki, et al., to appear in hep-lat
27. S. Necco, R. Sommer, Nucl. Phys. B **622**, 328 (2002)
28. K.G. Chetyrkin, B.A. Kniehl, M. Steinhauser, Phys. Rev. Lett. **79**, 2184 (1997)